AN ALTERNATIVE METHOD FOR HORIZONTAL & MULTILATERAL PRESSURE TRANSIENT ANALYSIS

C.L. Jordan, *JSW Innovations/ BOE Solutions,* **B.Waeyen***, PetroClass Inc.*
C.R. Smith, *SemCams*, **R. Jackson,** *BOE Solutions Inc.*

This paper was presented at the Offshore Mediterranean Conference and Exhibition in Ravenna, Italy, March 25-27, 2009. It was selected for presentation by the OMC 2009 Programme Committee following review of information contained in the abstract submitted by the authors. The Paper as presented at OMC 2009 has not been reviewed by the Programme Committee.

ABSTRACT

Traditionally pressure transient analysis is limited to simple wellbore completions such as stimulated vertical wells or horizontal completions with the complexity of a single monobore. For problems with greater geometrical complexity, numerical or highly computationally challenging solutions are normally can implemented. Yet, the execution of complex wells (due to higher productivity, and despite higher costs and more complex drilling and completion procedures) including multilaterals is becoming increasing more common in unconventional resource plays such as tight or shale gas/oil and of course offshore completions. As a result, there is a need for sophisticated models, but not at the penalty of additional computational power. To address such a need, this paper presents a simple semi-analytical model that allows for the pressure description of complex well designs, including horizontal and similar well completions.

The new procedure uses a series of sources/sinks to model well designs including horizontal wells with multistage transverse fractures. The procedure is robust such that it honours the early-time transient behaviour generated by other mathematically complex (but geometrically limited) solutions, while maintaining flexibility for use with non-conventional completions. As an artifact of procedure, the procedure also condenses to simple partial and fully penetrating vertical well solutions which allows for a semi-unified modeling process for a variety of scenarios. Discussion of adaptation for anisotropy and multiple well systems will also be included. The procedure is validated against results from traditional synthetic and numerical well testing solutions, as well as some field data.

This approach also allows for visualization of the pressure distribution beyond the well into the greater reservoir, and is easy amendable from pressure to rate forecasting. Overall, the procedure provides an efficient means for the approximate modeling for the pressure behavior of non-conventional wells, and can be applied to oil or gas systems, as well as coal or shale gas.

INTRODUCTION

Most sealed reservoir solutions (i.e. no-flow boundaries at the far field boundary condition) are obtained by integration of the appropriate Green's function leading to solutions with sums of single, double, and triple infinite series, whose convergence is particularly slow around the wellbore (although numerical integration reduces the computing time considerably)[1,2]. Other approaches have been developed using boundary element theory, as demonstrated by Cheng[3], but generally require evaluation of singular integrals. In most cases, the boundary condition is that of uniform flux along the length of the well[A].

[A]Butler *et al*[4] considers uniform flux to be a poor assumption, and states the assumption of uniform flux would result in pessimistic productivity predictions. A review of the investigation showed productivities differed by a factor 1.2 and slightly higher[4]. Chen *et al*[5], states the difference decreases as vertical permeability decreases and/or skin factor increases.

In this study, in order to generate a model for horizontal and/or multilateral wells, within arbitrary shaped bounded reservoirs, an approximate (but computationally efficient) transient solution is generated initially, and then coupled to boundary model which is generated independently. This procedure can be applied to both uniform flux and constant pressure wellbore conditions[B], and is computationally more efficient and versatile then previous methods (and is non-numerical).

Instead of analytically or numerically integrating a Green's or similar function along the path of interest, the transient solution is simply based on the summation of individual partial penetrating (PP) solutions – a much simpler solution than those presented by Thompson[2] or others. In this study, the dimensionless PP Laplace solution given by Bui *et al*[7] (and Slimani *et al*[8]) was implemented (Appendix A[C]). The solution is simply superimposed "*n*" times where "*n*" is determined by dividing the horizontal length of interest "L_w" by the assumed wellbore radius of for the PP well. The generic (or final total) Laplace solution is then given by superimposing all the partial penetration wells.

METHODOLOGY: TRANSIENT PERIOD

For the approximate uniform flux solution, the total volumetric flow rate of the horizontal well is distributed evenly over the "*n*" PP wells. In this scenario, the solution predicts that well pressure varies along the well with the highest pressure drop at the center and decreasing towards the ends[9]. For the constant pressure wellbore condition, the solution can be generated by specifying a system of equations resulting in a matrix problem as shown in Appendix B. Generally speaking, the PP wells are superimposed on each well in the system and flowing pressure specified. This means that each row of the matrix represents a single well (i.e. observation point) while each column represents the other wells impact. This matrix is then solved for the rate at each well required for the specified flowing pressure – the individual well rates are then summed for the total well rate. This operation is repeated at various times to get a rate profile as a function of time.

Both the approximate uniform flux and constant pressure solutions are in Laplace space, and need to be inverted to real space. To improve the speed of the solution[D], numerical inversion of the solution to real space from Laplace was not performed using the traditional Stefhest alogorithm[10]. Alternatively, an approach inspired by the work of Bourgeous[11], allowed for the easy inversion of the approximate uniform flux solution by simply using $p_D(t_D)=p_D(s)\times(s)$ where $s = 1/t_D$, and t_D is the dimensionless time of interest. In his investigation, Bourgeois[11] did not directly claim that this aforementioned calculation could be used to invert Laplace solutions, but a comparison of real and Laplace asymptotes for constant rate drawdown in an infinite acting reservoir reveal a simple analytical relationship. A similar procedure can be obtained for constant flowing pressure scenario. Using Jacob and Lohman's[12] long time approximation for the dimensionless flow rate at a well, Laplace and real space solutions can be evaluted implying $q_D(t_D)= q_D(s)/s$ where $s = 1/t_D$, and t_D. Appendix C outlines the inversion of the Laplace solutions for the approximate uniform flux solution, and the constant pressure solution[E].

Figure 1 shows the inversion of the solution for a single well in the center of a closed reservoir using both Stefhest[10] and the proposed non-numerical method inspired by

[B] For this study, the pressure drop along the horizontal well (i.e. frictional losses) will be ignored as this only becomes important when wellbore flow rate is high, and the reservoir drawdown is low (which, as illustrated by Hill *et al*[6] tends to occur in high permeability reservoirs with long horizontal wells, and small wellbore diameters).

[C] Significant testing showed that the infinite summation term in equation (1), Appendix A, can be efficiently approximated with only 75 terms, and remained at this value for the remainder of the work.

[D] Performing calculations in Laplace removes the convolution/superposition nature for constant pressure forecasts also improving speed of calculations.

[E] Similarly, Schapery[35] showed that if radial flow exists, then the inverse of the Laplace transformation can be approximated by $p_D(t_D)=p_D(s)\times(s)$ where $s=0.5/t_D$. Later, Najurieta[13] introduced an improved Schapery technique in which the Laplace parameter materializes in the form of $s=1/(\gamma t_D)$. These similar approaches (including the complex inversion formula[14]), were not found to be satisfactory for all time domains, particularly pseudo-steady-state.

Bourgeois[11]. Although the results indicate that the solution is suitable for radial flow, the approximation is poor for dual porosity (assuming the classic Warren & Root[15] model). Figure 2 shows the Stefhest[10] and Bourgeois[11] approximation for a dual porosity scenario for an interporosity coefficient and storativity ratio of 1E-6 and 1E-1, respectively[F].

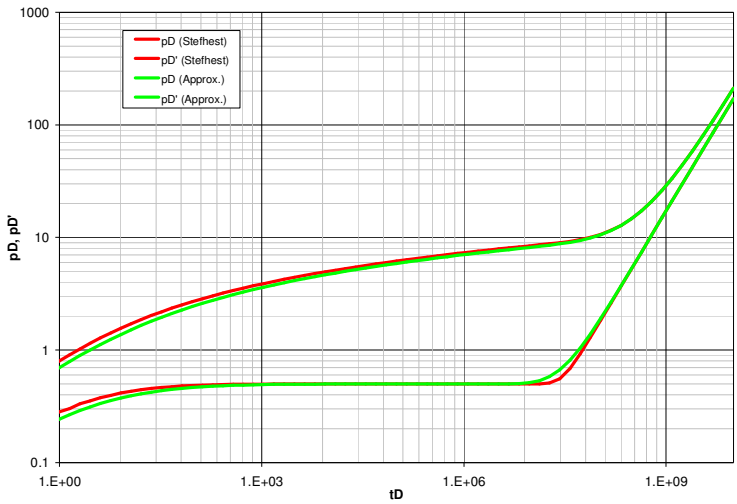

Figure 1: Laplace Space Inversion Using Approx. Method

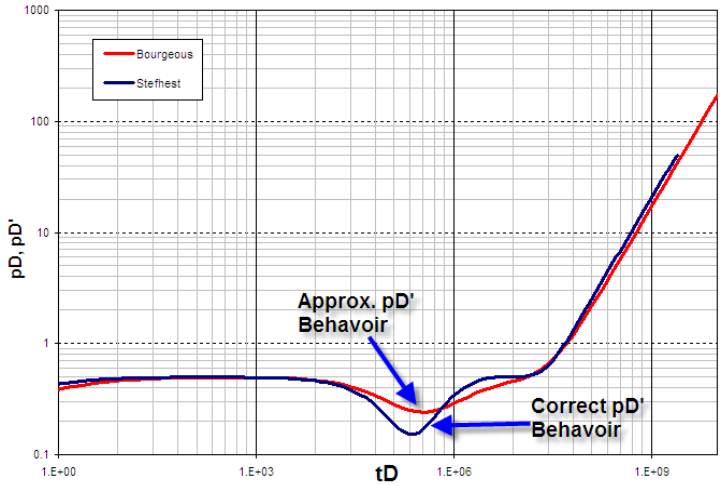

Figure 2: Laplace Space Inversion Using Approx. Method (Dual Porosity Example)

To test the proposed PP solution for modelling horizontal wells, a number of type curves were generated and validated against commercial software (which implemented he solution presented by Thompson *et al*[2] and assumes a uniform flux solution). In these examples, horizontal lengths were varied from 200 to 1000m (656 – 3280 ft), with a horizontal permeability of 10 md, and a vertical permeability of 1 md. A net pay of 5m (16.404 ft) was assumed, while the perforated interval (h_w) was set to $2r_w$. Figure 3 shows the dimensionless pressure and pressure derivatives respectively, associated with these test cases. In these examples, p_D and t_D are based on the average horizontal permeability $(k_x k_y)^{0.5}$ as opposed to the $k = (k_z k_x k_y)^{1/3}$.

To continue testing, production forecasts were generated assuming single phase oil using both the approximate uniform flux solution and the constant pressure solution. The forecast was based on the rock and fluid properties of u_o = 2.6688 cp, β_o=1.151, c_t=1.388x10^{-5} psia^{-1}, h = 16.4 ft, ϕ = 10%, t_f = 120 ^{o}f, S_w = 20%, k_v = 1 md, and k_h = 10 md. The horizontal well length and wellbore radius was set to 152 m (500 ft), and 0.152 m (0.5 ft), respectively.

[F] Small error is also evident when wellbore storage is included (not shown).

Initial pressure was set to 1,400 psia while flowing BHP was specified to be 200 psia. These forecasts, shown in Figure 4, assume an infinite reservoir scenario (i.e. no constant pressure or no-flow boundaries at the far field boundary condition in horizontal plane).

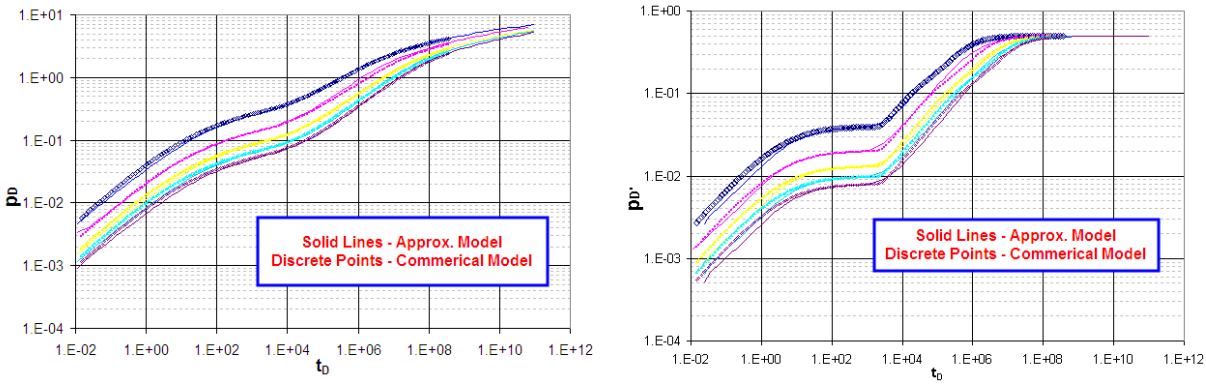

Figure 3: Pressure & Pressure Derivative Comparison (Approx Uniform Flux Model)

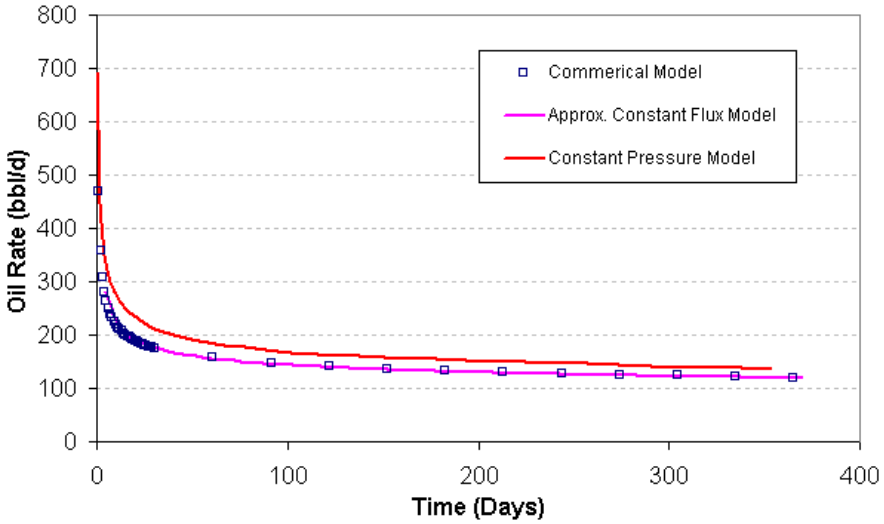

Figure 4: Deliverability Comparison (Single Lateral Example)

As additional testing, rate forecasts were generated for a dual lateral system as shown in Figure 5. In this scenario, both laterals are completed within the same zone, and are 82 m (269 ft) and 64 m (210 ft) length respectively for a total of 146 m (481 ft). Given the assumed wellbore radius of 0.152 m (0.5 ft) for the partially penetrating vertical wells, approx. 1000 wells were used to mimic the multilateral well.

Similar to the single well forecast, the dual lateral forecast was based on the rock and fluid properties of u_o = 2.6688 cp, β_o=1.515, c_t=1.388x10^{-5} psia^{-1}, h = 16.4 ft, ϕ = 10%, t_f = 120 ^{o}f, S_w = 0%, k_v = 1 md, and k_h = 10 md. Initial pressure was set to 1,400 psia while flowing BHP was specified to be 200 psia. Again, no reservoir boundaries were incorporated into the model as this stage. The results of the approximate model were then compared to those of a dual lateral system created using a commercial simulator, which used unstructured grids with automated 3-D refinements to capture flow geometry around the wellbore (Figure 5). Production forecasts using the approximate uniform flux, the constant pressure, and numerical solutions are shown in Figure 6.

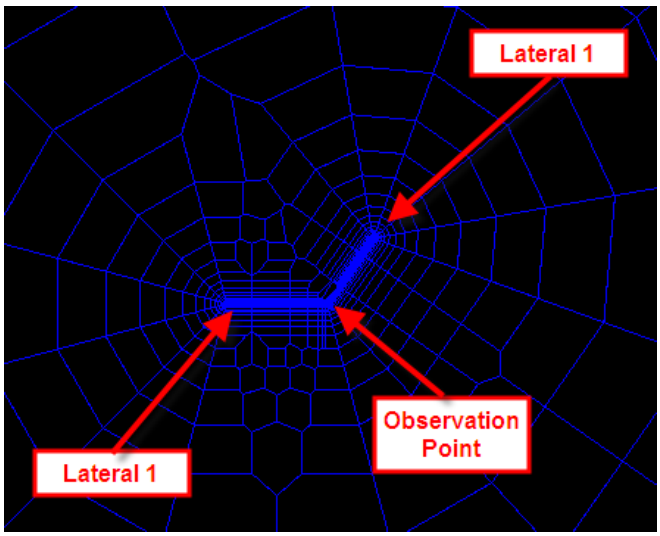

Figure 5: Dual Lateral Example (Unstructured Gridding)

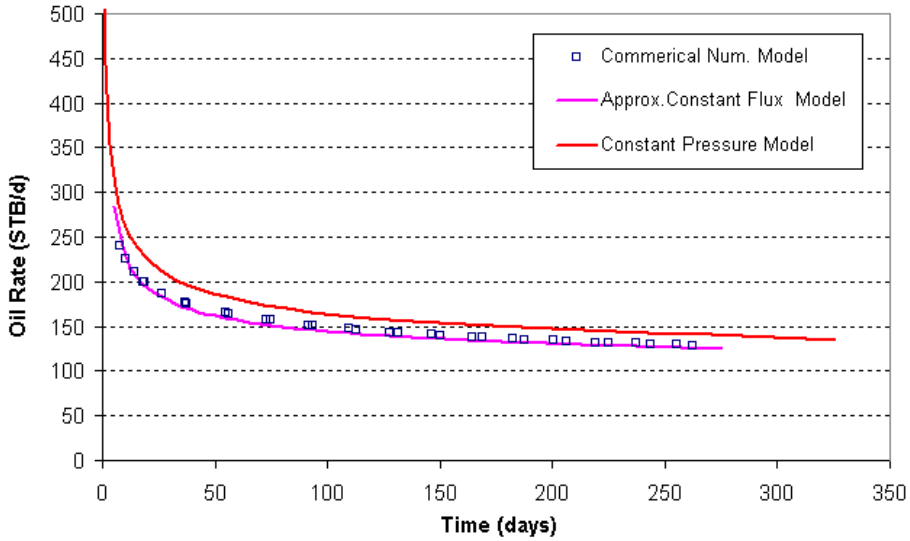

Figure 6: Production Forecast (Dual Lateral Example)

Using an approximate deconvolution process, the numerical rate forecast and the constant pressure solution using PP wells was converted to equivalent constant rate drawdown scenario for type curve comparison with the uniform flux solution. First, the rates are converted to dimensionless form and the reciprocal evaluated for p_D as shown in Appendix D, and the results plotted against dimensionless material balance time (as opposed to time) as introduced by Blasingame *et al*[16] . As a result, the constant rate type curves for the constant pressure solution and numerical model can be compared to the uniform flux type curve as shown in Figure 7. As can be seen from the results, the early-time match is poor, most likely due to inaccuracies in the numerical gridding, but the mid and late-time regions are very comparable.

METHODOLOGY: PSEUDO-STEADY-STATE (PSS) COUPLING

To generate boundaries, a process based on an approximation of the common image well procedure is used, and was inspired by Caudle[17], Jankovic[18], Lin[19], Leblanc[20], and others who used this approach for steady-state and PSS problems. In this process, *pseudo image*[G], or "fake", wells were arbitrarily placed and their coefficients (or rates) adjusted to achieve desired boundary conditions for the real wells. The theoretical justification of this work is

[G] For practicality, the wells are called "pseudo" image wells as they are not true mirror images of any real physical well (or another image well).

based on superposition and summarized by Bear[21] who stated that any linear combination of solutions to a homogeneous linear partial differential equation (PDE) is also a solution to the that same PDE [H] (refer to Appendix E).

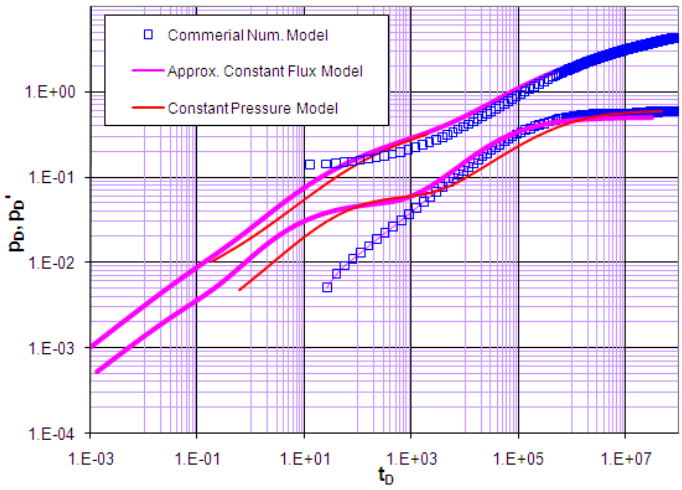

Figure 7: Constant Rate Drawdown Type Curves (Dual Lateral Example)

In this study, a small fixed number of pseudo image wells (i.e. 60) are chosen and arbitrary placed outside the reservoir, and then rates determined such that an equal potential existed at a number of collocation or test points along the desired boundary location. The solution process becomes a matrix problem as the rates at all pseudo image wells need to be determined simultaneously while evaluating the boundary conditions at test points. It is important to note the size of the matrix is reasonable compared to finite difference and finite element methods due the reduction in the dimensionality of the problem (no domain gridding is required). In other words, during the matrix operations, the normal potential is evaluated at a number of test points located along the boundary, and the image well rates calculated to ensure that difference was zero across the boundary. After the pseudo image wells rates are calculated, then total compiled solution is generated by superimposing the real and pseudo images wells. Appendix F and G algebraically illustrate the compiled solution and the normal derivative process, respectively.

In solving for the coefficients (C_n) of the pseudo image wells, an M x N matrix results, where N represents the number of image wells, and M represents the number of test points along the desired reservoir boundary. If there are more test points than pseudo image wells, the solution is met in an average sense and can be solved using least squares reduction or other matrix solution processes[I]. The procedure is then repeated for each additional real well in the system, and then superimposed to generate a multi-well bounded solution from a solution for multiple wells in an infinite acting reservoir.

For testing purposes, a type curve was generated by Rattu[22] with a numerical model using geometrically spaced grids for both areal and radial grids for a closed homogeneous reservoir. Figure 8 shows good comparison, for transient and PSS flow, between the pressure solutions obtained by the numerical and pseudo-image approach. For comparison, the well known analytical solution developed by van Everdingen and Hurst[23] is also included.

[H] In traditional applications for reservoir engineering, these solutions and their coefficients manifest themselves as image wells where the coefficients are known a prior since the spatial locations of image wells are chosen such that they are truly mirror images (both rate and location) of the real physical wells. Subsequently, it is well known that for multiple boundaries, there is a mirror effect between the image wells resulting in "images of image wells". As a result, without any consideration to varying rate schedule or multiple wells, generating a suitable solution for a single well in somewhat irregular shaped reservoir becomes a fairly tedious task due to calculating the large number of image wells (and their respective positions). In many instances, infinite summations of image wells are theoretically are required to ensure a stable solution

[I] If M = N, the solution is met exactly at the test points with little or no control at boundary positions in between the test points. Testing showed a 2:1 ratio of test poitns to pseudo image wells provides the best results. Caudle[17], Jankovic[18] and Lin[19] present an excellent summary of matrix operations.

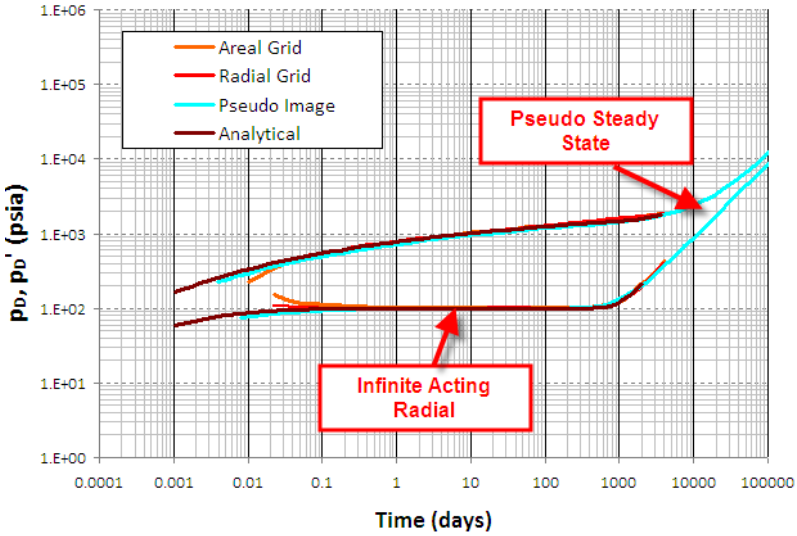

Figure 8: Validation of Boundary Conditions Using Pseudo-Image Method

An interesting advantage of the pseudo-image method is that there is no need to consider the impact of gridding on early-time behavior (the method is not discretized within the domain). Also, once the number of test points has been specified, then the amount of computational effort is only proportional to the number of test points required to generate the desired geometry. A practical advantage is that irregular shaped reservoir models can now be implemented easily - a situation in which horizontal and multilateral wells are particularly suited since they provide better vertical and areal sweep for odd-shaped reservoirs[24]. Also, for long-term deliverability, the same rate forecasting algorithm used for conventional analytical solutions can be implemented, and evaluation of inflow performance of horizontal or multilateral wells in closed systems can be easily evaluated (without some of the more computational challenges indicated by Umnuayponwiwat et al[25]).

As a computational alternative to evaluating the normal derivatives for all the partial penetration wells of the horizontal well, the procedure could be performed for a single vertical well, and the principle of desuperposition[J] used to add the horizontal and/or multilateral effect. Desuperposition is defined as modifying known p_D values to p_D's for different systems. The approach may be used for any drainage shape and well location. For example, to compute the pressure behavior, p_D, for a well located in the center of square with wellbore storage and skin, simply a) compute the pressure disturbance for the same system without wellbore storage ($c_D = 0$), b) remove (subtract) the solution for a single well in an infinite system (with zero wellbore storage or skin), and c) add the solution for well, including wellbore storage and skin, in an infinite system.

To show that desuperposition was a suitable approach, the wellbore pressure profile was generated analytically for a well located in the center of the radial composite system according to solution presented by Ambastha[30]. Using the solution presented by Johns *et al*[31], wellbore skin and a positive skin were added in Laplace space, and then compared to a scenario in which wellbore storage and skin were added using desuperposition. Figure 9 shows a comparison of the solutions. Note, the value of c_D was chosen such that wellbore storage dominated a significant amount of the entire data set. These combinations of variables may unrealistic, but the example does illustrate that procedure is accurate and robust when compared to analytical procedures.

[J] Although by definition, the methodology is still superposition of linear solutions, it is called desuperposition in this paper to be consistent with the work presented by Gringarten, Ramey, and Raghavan[26], Chen and Brigham[27], Argawal[28], and Earlougher[29].

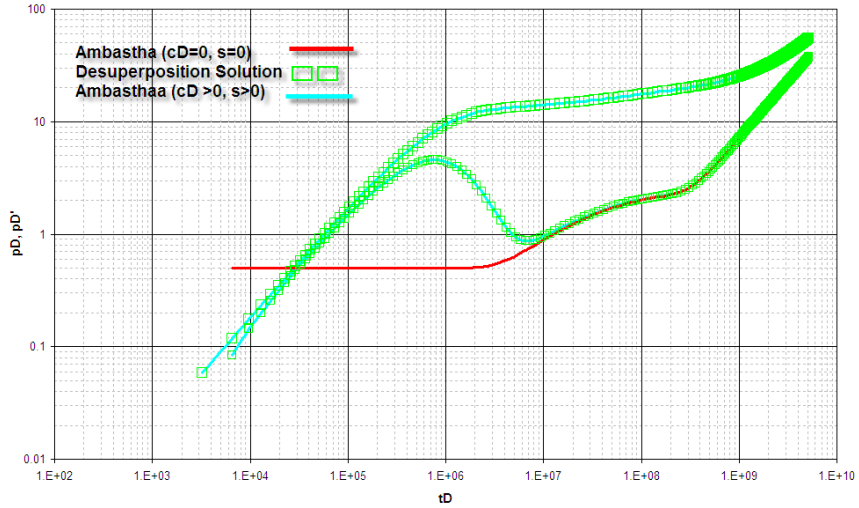

Figure 9: Desuperposition Validation (Composite Reservoir Example)

Considering the dual lateral example previously discussed, the reservoir size is now fixed to square area of 2,500 ft x 2,500 ft, which has an equivalent radial drainage radius "r_e" of 1410.474 ft. A constant pressure rate forecast was generated with the numerical simulator and the PP constant pressure solutions. The infinite acting type curves were then generated for the approximate uniform flux model, and the constant pressure models, and boundaries added using the pseudo-image well method and desuperposition. Finally rate forecasts for the two bounded solutions using PP was then generated. The deliverability forecast for all three scenarios are shown in Figure 10, and the type curve comparison is shown in Figure 11.

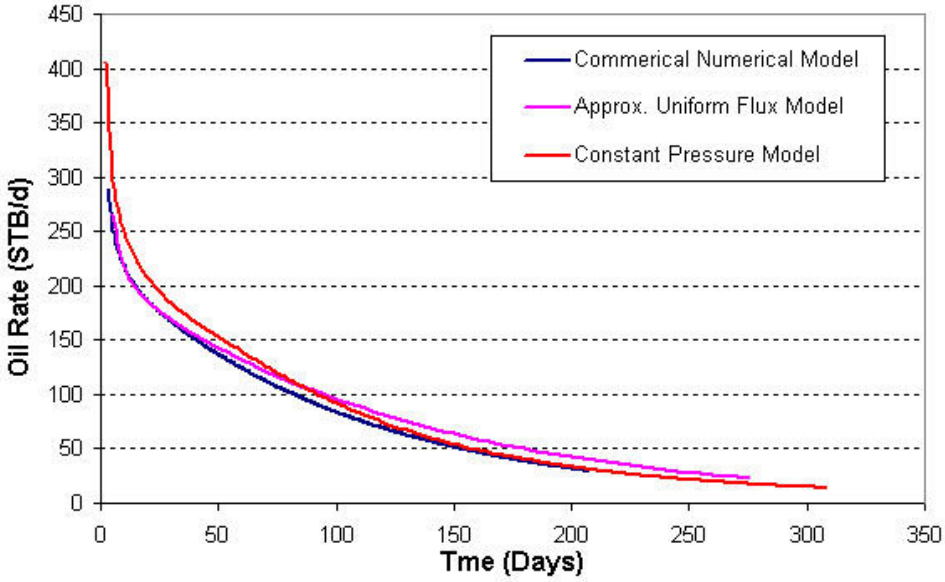

Figure 10: Production Forecast (Dual Lateral Example, Bounded Reservoir)

As a final test, solutions were generated for a dual lateral scenario within an arbitrarily shaped reservoir (refer to Figure 12). The laterals lengths are 500 m (1640 ft) for the east-west lateral, and 250 m (820 ft) for the north-south lateral. All other reservoir fluid and rock properties remained consistent with the previous example. Figure 13 shows the deliverability forecasts for the numerical, the approximate uniform flux, and the constant pressure models. As can be seen from the forecasts, the solutions based on the PP approach (whether uniform flux or constant pressure inner boundary conditions), provides a suitable match with the numerical models.

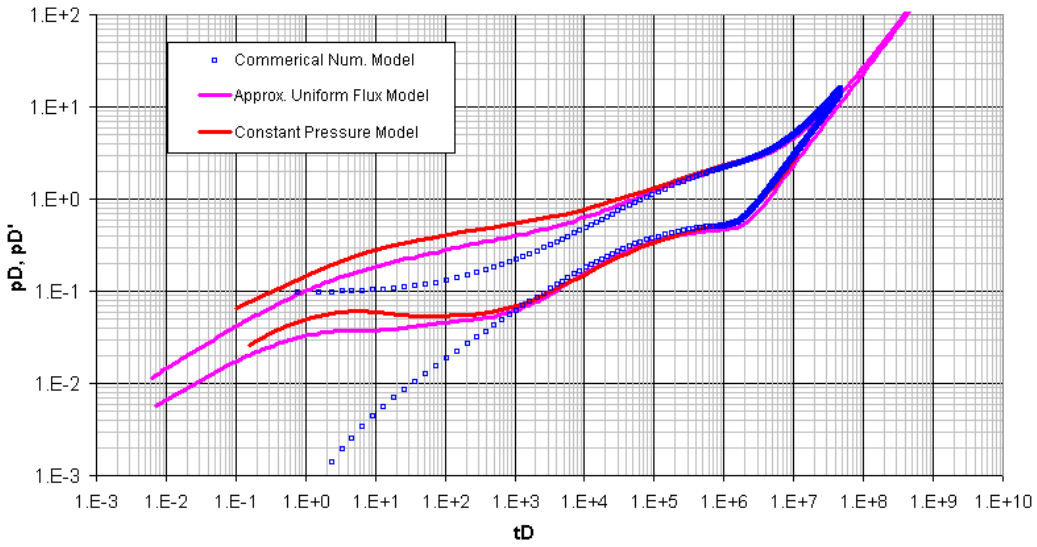

Figure 11: Type Curves Comparison (Dual Lateral Example)

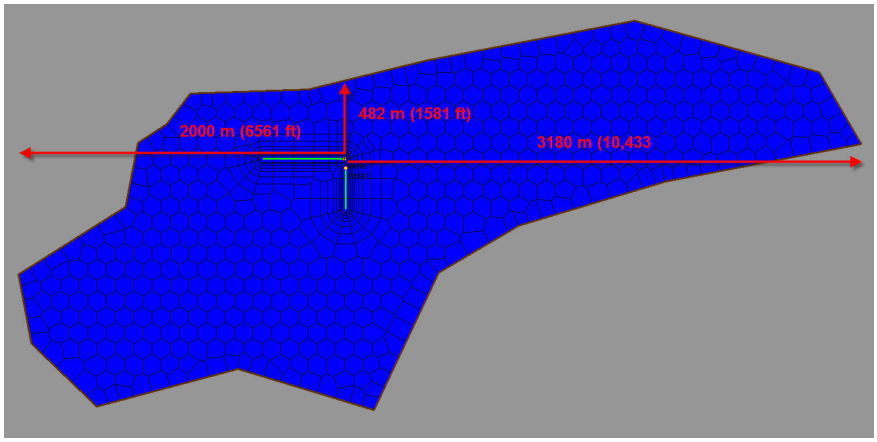

Figure 12: Reservoir Geometry (Arbitrary Shape Reservoir Example)

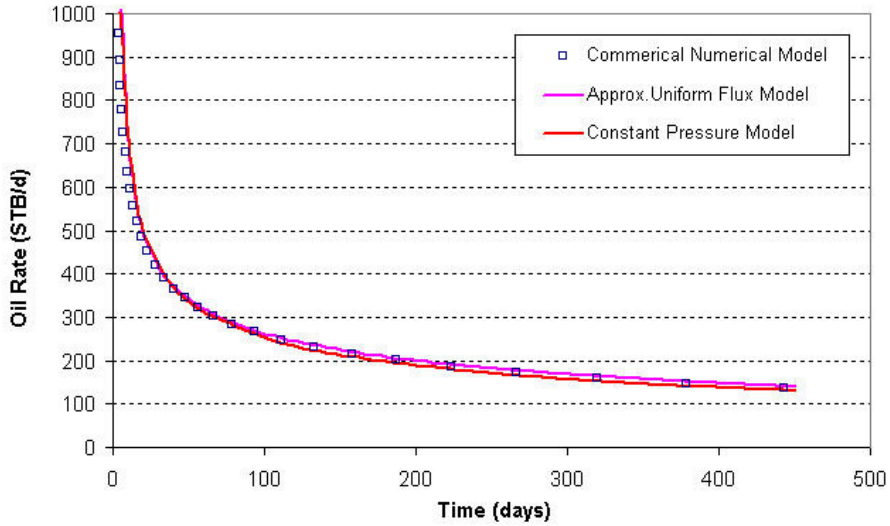

Figure 13: Production Forecast (Arbitrary Shape Reservoir Example)

CONCLUSIONS AND FUTURE WORK

A methodology of calculating horizontal well (single or multiple well configurations) performance in arbitrarily shaped reservoirs based on simple superposition of analytical partial penetration solutions, has been introduced. This approach is general (and readily

reproduces well known analytical solutions), and can be used for transient or PPS flow periods. Numerical testing has validated the more complex problems which are not available in analytical solutions. Additional testing will continue including validation against the classic Borisov[36] model, and more detailed numerical simulation.

Although not shown, the work can be extended to conventional and unconventional dry gas situations (including shale gas, and coal bed methane). By replacing the time and pressure variables in the dimensionless definitions, the prediction of long-term gas production can be accurately performed[33]. Germani *et al* shows the adaptation of the typecurve process for dry shale/CBM reservoirs with equilibrium desorption[34].

The work can also be extended to natural fractures in Laplace space by replacing the Laplace parameter with "$s \times f(s)$" in the Bessel functions. f(s) can be one of many natural fractures solutions including the Kazemi-de Swaan model[32], or the popular Warren and Root[15] model.

Furthermore, wellbore storage and skin can also be easily added to the solution as presented in many sources including Johns *et al*[31]. If applied to the individual well, a model with variable skin along the length of the horizontal well or multi-lateral can be generated for heterogeneous damage problems as discussed by Furui *et al*[37] (if applied to the total or compiled solution, then the skin would be distributed evenly along the well). Finally, horizontal anisotropy can also be included by using the common/appropriate scaling factors for x and y coordinates based on degree of anisotropy.

NOMENCLATURE

b	Penetration ratio, dim.
B_o	Oil Formation Volume Factor, dim.
C_D	Wellbore storage coefficient, dim.
C_n	Weighting coefficient, dim.
c_t	System compressibility, $psia^{-1}$
k	Reservoir permeability, md
h	Net pay, ft
h_b	Bottom non-open interval length, ft
h_w	Well open interval, ft
L_w	Horizontal well length, ft
P	Pressure, psia
P_i	Initial reservoir pressure, psia
P_D,	Wellbore pressure, dim.
P_D'	Wellbore pressure derivative w/r $\ln(t_D)$, dim.
P_{wcD}	P_D include storage/skin, dim.
q_D	Oil rate, dim.
r_D	Radius/Observation point, dim.
r_e	Reservoir drainage radius, ft
s	Laplace parameter
S_T	Skin Factor, dimensionless
μ_0	Oil Viscosity, cp

REFERENCES

1. Issaka, M.B., and Ambastha, A. K., "Drawdown and Buildup Pressure Derivative Analyses for Horizontal Wells", paper SPE 24323, SPE Rocky Mountain Regional Meeting, Casper, Wyoming, May 18-21, 1992.
2. Thompson, L. G., Manrique, J. L., and Jelmert, T. A., "Efficient Algorithms for Computing the Bounded Reservoir Horizontal Well Response", paper SPE 21827, Rocky Mountain Regional Meeting and Low Permeability Reservoir Symposiums, Denver, Colorado, April 15-17, 1991.

3. Cheng, Y., “Pressure Transient Testing & Productivity Analysis for Horizontal Wells”, Ph.D. Thesis, Texas A&M University, August 2003.
4. Butler, R.M., and Suprunowicz “A Comparison of Uniform Wellbore Flux and Constant Flux Wellbore Pressure Models for Horizontal Well Productivity Predictions”, Paper No. CIM 94-62, CANMET International Conference on Recent Advances in Horizontal Well Applications, March 20-23, 1994, Calgary, Canada.
5. Chen, H-Y, and Assad, N., “Horizontal-Well Productivity Equations with Both Uniform-Flux and Uniform Pressure Wellbore Modes”, paper SPE 97190, presented at the 2005 Annual Technical Conference and Exhibition, Dallas, Texas, USA, 9-12 October 2005.
6. Hill, A.D., and Zhu, D., “The Relative Importance of Wellbore Pressure Drop and Formation Damage in Horizontal Wells”, paper SPE 100207, presented at the 2006 Europec/EAGE Annual Technical Conference and Exhibition, Vienna, Austria, 12-15 June.
7. Bui, T.D, Mamora, D.D., and Lee, W. J., “Transient Analysis for Partially Penetrating in Naturally Fractured Reservoirs”, paper SPE 60289 presented at the 2000 SPE Rocky Mountain Regional/Low Permeability Reservoirs Symposium and Exhibition held in Denver, Colorado, 12-15 March 2000.
8. Slimani, K., Tiab, D., and Moncada, K., “Pressure Transient Analysis of Partially Penetrating Wells in a Naturally Fractured Reservoir”, paper SPE 104059, presented at the First International Oil Conference and Exhibition in Mexico, Cancun, 31 August – 2 September 2006.
9. Economides, M. J., Brand, C.W., and Frick, T. P., “Well Configurations in Anisotropic Reservoirs”, paper SPE 27980, presented at the 1994 Tulsa Centennial Petroleum Engineering Symposium, Tulsa, 29-31, August.
10. Stefhest, H., “Numerical Inversion of Lipike Transforms”, Communications of the ACM (Jan. 1970), **13**, No. **1**, 47-49.
11. Bourgeois, M., “Well Test Interpretation Using Laplace Space Typecurves”, Elf Aquitaine, April 1992.
12. Urajet, A. A., “Transient Pressure Response in a Cylindrical Reservoir Produced By a Well at Constant Bottom-Hole Pressure”, Ph.D Thesis, The University of Tulsa, 1979.
13. Najurieta, H.L.,: “A Theory fore Pressure Transient Analysis in Naturally Fractured Reservoirs”, JPT, (July, 1980), p. 1241-1250.
14. Cox., D “Solution of Unsteady Flow Problems in Porous Media”, PE 5980, Course Notes, Colorado School of Mines.
15. Warren, J.E., and Root, P.J., “The Behavoir of Naturally Fractured Reserviors”, paper SPE 426 presented at the Fall Meeting of the1962 Society of Petroleum Engineers, Los Angeles, 7-10 Oct.
16. Blasingame, T.A., McCray, T. L., and Lee, W. J., “Decline Curve Analysis for Variable Pressure Drop/ Variable Flowrate Systems”, paper SPE 21513, presented at the Gas Technology Symposium, Houston, Texas, January 23-24, 1991.
17. Caudle, B .H. “Mechanics of Fluids in Permeable Media”, Course Notes, University of Texas at Austin, 1996.
18. Jankovic, I., “High-Order Analytic Elements in Modelling Groundwater Flow”, Ph.D Thesis, University of Minnesota, 1997.
19. Lin, J. “An Image Well Method for Bounding Arbitrary Reservoir Shapes in the Streamline Model”.
20. LeBlanc, J. L.: “A Streamline Model For Secondary Recovery” paper SPE 2865 presented at the 1970 Ninth Biennial Production Technique Symposium, Wichita Falls, 14-15 May.
21. Bear, J., “Dynamics of Fluids in Porous Media”, Dover Publications Inc., New York, 1972.
22. Rattu, B. C.: “Modelling Techniques for Simulating Well Behaviour” M.Sc. Thesis, Texas A&M, May 2002.
23. van Everdingen, A.F., & Hurst, W., “Application of the Laplace Transformation to Flow Problems in Reservoirs”, Trans, AIME (1949), 186, 305-24.
24. Nunsavathu, U. N., “Productivity Index of Multilateral Wells”, M.Sc. Thesis, West Virgina University, 2006.

25. Umnuayponwiwat, S., and Ozkan, E., “Evaluation of Inflow Performance of Multiple Horizontal Wells in Closed Systems”, Journal of Energy Resources Technology, March 2000, Vol 122. Pages 8 – 13.
26. Gringarten, A, C., Ramey, H.J., Jr., and Raghavan, R., “Unsteady-State Pressure Distributions Created by a Well With a Single Infinite-Conductivity Vertical Fracture” Soc. Pet. Eng. J. (Aug. 1974) 347-360; Trans., AIME, 257.
27. Chen, J., & Bingham, W.E., “Pressure Buildup for a Well With Storage and Skin in a Closed Square”, SPE-AIME, 44th Annual California Regional Meeting, SPE Paper No. 4890, April 4-5, 1974.
28. Argawal, R.G., “A new Method to Account For Producing Time Effects When Drawdown Type Curves Are Used to Analyze Pressure Buildup and Other Test Data”.
29. Earlougher, R.C., Jr., Ramey, H.J., Miller, F.G., and Meuller, T.D., :“Pressure Distributions in Rectangular Reservoirs”, J. Pet. Tech., February 1968, 199-208; Trans., AIME, 243.
30. Ambastha, A.K.: “Pressure Transient Analysis for Composite Systems”, Ph.D. Dissertation, Stanford University, Stanford (1988).
31. Johns, R.T., and Ma, L., “Effect of Pretest Pressures and Temperature on DST Interpretation”, paper SPE 51255, presented at the 1997 Annual Technical Conference and Exhibition, San Antonio, Texas, 5 – 8 October.
32. Kazemi, H., “Pressure Transient Analysis of Naturally Fractured Reserviors”, Trans, AIME 256 (1969), pages 451-461.
33. Mattar, L. “Tech Talk: Pseudo-Time or Pseudo-Pressure”, Fekete Newsletter. Winter 2001.
34. Germani, S., Pooladi-Darvish, M., Morad, K., and Mattar, L., “Type Curves for Dry CBM reservoirs with Equilibrium Desorption” Journal of Canadian Petroleum Technology, July 2008, Volume 47, No. 7.
35. Schapery, R.A.: “Approximate Methods of Transform Inversion for Viscoelastic Stress Analyis”, paper presented at the Fourth U.S. National Congress of Applied Mechanics (1961), p. 1075-1085.
36. Joshi, S.D., “A Review of Horizontal Well and Drainhole Technology”, paper SPE 16868. Presented at the 62th Annual Technical Conference. Dallas, TX, September 27-30, 1987.
37. Furui, K., Zhu, D., and Hill, A., “A Rigorous Formation Damage Skin Factor and Reservoir Inflow Model for a Horizontal well”, paper SPE 74698 presented at the SPE International Symposium and Exhibition on Formation Damage, Lafayette, Louisiana, 20-21 February 2002.

APPENDIX A: PARTIAL PENETRATION MODEL

The dimensionless partial penetration (PP) Laplace solution given by Bui *et al*[7], as well as Slimani *et al*[8] is shown below in (1)

$$\overline{p_D}(s, r_D) = \frac{K_0(\sqrt{s} r_D)}{s\sqrt{s} K_1(\sqrt{s})} + \frac{1}{s}\frac{2}{b^2}\sum_{n=1}^{\infty} \frac{\Gamma}{n^2\pi^2\sqrt{s+\zeta^2}} \frac{K_0(\sqrt{s+\zeta^2} r_D)}{K_1(\sqrt{s+\zeta^2})} \tag{1}$$

“*b*” is the penetration ratio, and dimensionless radii are defined as below in (2) and (3). h_w represents the perforated interval in the partial penetrating model, while “*r* “ represents the observation point.

$$b = \frac{h_w}{h} \tag{2}$$

$$r_D = \frac{r}{r_w} \tag{3}$$

The remaining parameters "ζ", "h_{bd}" and "Γ" are given in (4), (5) and (6). Note, h_b is the bottom non-open interval length (i.e. the amount of the net pay not perforated, completed below the open interval in the vertical partial penetrating model).

$$\zeta = \frac{n\pi}{h_D} \tag{4}$$

$$h_{bD} = \frac{h_b}{h} \tag{5}$$

$$\Gamma = \left[\sin\left(n\pi\left(h_{bD}+b\right)\right) - \sin\left(n\pi\left(h_{bD}\right)\right)\right]^2 \tag{6}$$

In real space, the dimensionless time and pressure definitions are defined as shown in (7a) and (7b) respectively.

$$t_D = \frac{0.0002637kt}{\phi\mu c_t r_w^2} \tag{7a}$$

$$P_D = \frac{kh(P_i - P_{wf})}{141.2q_oB\mu} \tag{7b}$$

To generate the horizontal or multilateral solution from equation (1) (whether assuming an uniform flux or constant pressure wellbore condition), each well is placed exactly side-by-side (but not overlapping) and superimposed according to (8). The relationship between the number of PP wells and horizontal well length is shown in (9).

$$\overline{p_{DT}(s)} = \sum_{i=1}^{n} p_D(s, r_{D_i})_i \tag{8}$$

$$n = \frac{L_w}{r_{w,pp}} \tag{9}$$

APPENDIX B: MATRIX SETUP FOR CONSTANT PRESSURE SOLUTION

The matrix below represents the solution process for the constant pressure solution. Each row represents a single, but unique, PP well in the array of PP wells. The remaining columns in each row represents the image of the remaining PP wells outside the PP well of interest. In this notation below, rD_{12} represents the impact of PP well 2 on PP well 1. Once all the rates are determined for each PP well, they are summed to provide the total well rate.

$$\begin{array}{ccccccc}
\overline{q_1(s)}\bullet\overline{p_D(s,r_{D11})}+ & \overline{q_2(s)}\bullet\overline{p_D(s,r_{D12})}+ & \overline{q_3(s)}\bullet\overline{p_D(s,r_{D13})}+ & .... & \overline{q_n(s)}\bullet\overline{p_D(s,r_{D1n})} = p_{D,spec} \\
\overline{q_1(s)}\bullet\overline{p_D(s,r_{D21})}+ & \overline{q_2(s)}\bullet\overline{p_D(s,r_{D22})}+ & \overline{q_3(s)}\bullet\overline{p_D(s,r_{D23})}+ & \dots & \overline{q_n(s)}\bullet\overline{p_D(s,r_{D1n})} = p_{D,spec} \\
\overline{q_1(s)}\bullet\overline{p_D(s,r_{D31})}+ & \overline{q_2(s)}\bullet\overline{p_D(s,r_{Dn2})}+ & \overline{q_3(s)}\bullet\overline{p_D(s,r_{Dn3})}+ & \dots & \overline{q_n(s)}\bullet\overline{p_D(s,r_{D1n})} = p_{D,spec} \\
\vdots & \vdots & \vdots & \vdots & \vdots \\
\overline{q_1(s)}\bullet\overline{p_D(s,r_{Dn1})}+ & \overline{q_2(s)}\bullet\overline{p_D(s,r_{Dn2})}+ & \overline{q_3(s)}\bullet\overline{p_D(s,r_{Dn3})}+ & \dots & \overline{q_n(s)}\bullet\overline{p_D(s,r_{Dnn})} = p_{D,spec}
\end{array}$$

APPENDIX C: LAPLACE SPACE INVERSION

A review of the Laplace and real space asymptotes for infinite acting radial flow time period, for constant rate drawdown, are nearly equivalent as illustrated by equations (10) and (11). Similar asymptotes can be evaluated for the constant flowing pressure condition as shown by equations (12) and (13). Based on symmetry, equations (14) and (15) can be used to invert

Laplace solutions for constant rate (uniform flux) and constant pressure conditions, respectively.

$$p_D(t_D) = \frac{1}{2}(\ln(t_D) + 2\ln(2) - \gamma) \tag{10}$$

$$\overline{s\,p_D(s)} = \frac{1}{2}(\ln(\tfrac{1}{s}) + 2\ln(2) - 2\gamma) \tag{11}$$

$$\frac{1}{q_D(t_D)} = \frac{1}{2}(\ln(t_D) + 2\ln(2) - \gamma) \tag{12}$$

$$\frac{s}{\overline{q_D(s)}} = \frac{1}{2}(\ln(\frac{1}{s}) + 2\ln(2) - 2\gamma) \tag{13}$$

$$p_D(t_D) = s \cdot p_D(s)_{s=\frac{1}{t_D}} \tag{14}$$

$$q_D(t_D) = \frac{q_D(s)}{s}_{s=\frac{1}{t_D}} \tag{15}$$

APPENDIX E: LINEAR COMBINATION OF LINEAR SOLUTIONS TO PDE

If p_{D1} is a linear dimensionless solution for a single well in an infinite reservoir, then $C_1 \times p_{D1}$ + $C_2 \times p_{D1}$ + .. $C_n \times p_{D1}$ is also a solution where C_1, C_2 … C_n are arbitrary constants adjusted such that the combination is a new solution to the same liquid diffusivity equation, but subject to different boundary conditions. Equation (18) algebraically illustrates this concept:

$$p_D = C_1(p_{D1}) + C_2(p_{D2}) \tag{18}$$

APPENDIX F: COMPILED SOLUTION

Once the coefficients of the pseudo-image wells have been evalutaed for desired boundary conditions, the total (or compiled) solutions is generated according to (19). The coeifficients C_n must be evaluated according to Appendix G to obtain the desired boundary conditions.

$$p_D = \sum_{i=1}^{n} C_n(p_{D,pseudo}) + p_{D,real} \tag{19}$$

APPENDIX G: NORMAL DERIVATIVES / EVALUATION OF COEFFCIENTS

Equation (20) algebraically represents the normal derivatives of (19), where x_{Do} and y_{Do} represent observation (or test) points on the boundary. The angle (α) is the boundary angle and is measured from the positive horizontal axis to the normal line. If C_n is adjusted such that (20) is satisfied, then a suitable boundary condition has been met.

$$\frac{\partial[p(y_D, x_D, s)_D]}{\partial n}_{Real} = \sum_{n=1}^{N} C_n \left[\left[\cos(\alpha) \frac{\partial[p(x_{Do}, s)_D]}{\partial x_{Do}} + \sin(\alpha) \frac{\partial[p(y_{Do}, s)_D]}{\partial y_{Do}} \right] \right]_{Pseudo} \tag{20}$$